11-1993

Sensitivity Improvement of a 1-μm Ladar System Incorporating an Active Optical Fiber Preamplifier

Michael S. Salisbury
Technology Scientific Services Inc.

Paul F. McManamon
U.S. Air Force

Bradley D. Duncan
University of Dayton, bduncan1@udayton.edu

Sensitivity improvement of a 1-μm ladar system incorporating an optical fiber preamplifier

Michael S. Salisbury*
University of Dayton
Center for Electro-Optics
300 College Park
Dayton, Ohio 45469-0226

Paul F. McManamon
Wright Laboratory
AARI-2, Electro-Optic Sensors Group
Wright-Patterson Air Force Base, Ohio
45433-6543

Bradley D. Duncan, MEMBER SPIE
University of Dayton
Center for Electro-Optics
300 College Park
Dayton, Ohio 45469-0226

Abstract. In an effort to increase the SNR of a continuous wave, 1-μm all solid state ladar system, a rare-earth-doped optical fiber amplifier is investigated as a preamplifier for ladar return signals. The experimental system is detailed and a theoretical analysis of the fiber amplifier's effect on both heterodyne and direct detection schemes is provided. Beginning with the optical powers incident on the detector, the signal and noises are analyzed, through the detector electronics, to predict the SNR. The SNR is then plotted as a function of the return signal power, and a SNR threshold is defined to determine a minimum detectable signal power. The return signals required to attain the SNR threshold are then compared for four cases: direct detection with and without the fiber amplifier and heterodyne detection with and without the fiber amplifier. For the direct detection scheme considered, our results predict a sensitivity increase of 20.6 dB with the addition of the fiber amplifier, yet for heterodyne detection the predicted sensitivity increase is only 3.1 dB.

Subject terms: acquisition; tracking; pointing; ladar; laser radars; fiber amplifiers; SNR.

Optical Engineering 32(11), 2671–2680 (November 1993).

1 Introduction

In remote sensing, the detection of weak return signals is of vital importance. One method of increasing the sensitivity of a remote sensing device, such as a ladar (laser detection and ranging) system, is to optically amplify the return signal before detection. Rare-earth-doped optical fiber amplifiers offer a compact and lightweight optical preamplifier for integration into a ladar system.

Mature solid state ladar technology exists for wavelengths of 1.064 μm, built around Nd:YAG laser sources. A solid state 1.064-μm ladar testbed has thus been constructed to evaluate the potential of experimental optical fiber amplifiers as components of a ladar system.[1] The primary fiber amplifiers developed by the telecommunication industry, however, are constructed using praseodymium- and erbium-doped fibers, for amplification at 1.3 and 1.55 μm, respectively.[2,3] Because these amplifiers will not amplify a 1.064-μm ladar return signal, they are of little use for our application. Fortunately, however, 1.064-μm laser sources have successfully been constructed using neodymium-doped (Nd^{3+}) optical fibers.[4,5] Configured as a fiber amplifier, this type of fiber will be shown to be appropriate for amplifying 1.064-μm ladar return signals, thus providing an innovative application of neodymium-doped fiber amplifiers to mature ladar technology.

*Current affiliation: Technology Scientific Services Inc., P.O. Box 3065, Overlook Branch, Dayton, Ohio 45431.

Paper TPA-17 received April 12, 1993; revised manuscript received June 1, 1993; accepted for publication June 15, 1993.

Our system can be configured for heterodyne detection or direct detection, allowing for comparisons between the two detection schemes. When the fiber amplifier is added to the ladar receiver, the return signal is increased by a power gain factor. However, spontaneous emission from the fiber amplifier adds an optical noise to the receiver, so the benefit of the gain must be weighed against the increased noise. In later sections, the added noise, consisting of a shot-noise term and several beat-noise terms, is examined in detail.

Direct detection ladar systems are limited by the noise generated by the detection electronics. In a simple, inexpensive system, these noises can be quite large. When the noise added by the spontaneous emission does not have a significant impact on the overall noise of the system, an increase in direct detection sensitivity is achieved by adding the fiber amplifier, as we show later.

For heterodyne detection, a large local oscillator (LO) power is mixed with the return signal to ensure that the detection is LO shot-noise limited. In this case, the spontaneous emission directly increases the shot noise. Also, the beat-noise term between the spontaneous emission and the large LO has a strong impact on the noise level. Overall, the sensitivity of a heterodyne ladar system will be shown to be minimally affected by the addition of a fiber amplifier.

In Sec. 2, an overview of the ladar system is given, and in Sec. 3 we discuss the experimental setup used to incorporate the fiber amplifier into the system. In Sec. 4, we derive the SNR for direct detection with and without the fiber amplifier, plotting the SNR versus the return signal power to give a measure of the sensitivity. In Sec. 5 we consider heterodyne detection with and without the fiber amplifier. Pre-

liminary experimental work is presented in Sec. 6, and in Sec. 7 we present an analysis and comparison of the theoretical results of Secs. 4 and 5.

Finally, to limit the scope of this article, only the rigorous theoretical analyses concerning the incorporation of an optical fiber amplifier into a ladar system are presented. The results of experiments we performed to verify our predictions will be included in a forthcoming companion article.

2 Ladar Overview

This section reviews in detail the ladar system used to test the performance of the neodymium-doped fiber amplifier. To begin, we discuss the general heterodyne and direct detection setup without the fiber amplifier. The heterodyne detection scheme is described first, followed by a discussion of the direct detection scheme.

Figure 1 shows the components of the heterodyne ladar system. The laser source is a Lightwave Electronics model 120-03 continuous wave (cw), diode-pumped, Nd:YAG laser with 40 mW of linearly polarized output at 1.064 μm. The laser cavity is a MISER configuration, giving a frequency stabilized output with a 5-kHz linewidth. This laser provides the power for both the local oscillator leg and the output signal. The beam then passes through an Electro-Optics Technology model 1845-5 Faraday optical isolator to prevent backscatter from other optical components in the system from reentering the laser head.

The local oscillator beam is split off using the combination of a half-wave plate in a rotatable mount and a polarizing beamsplitter cube. For linear polarization, the beamsplitter transmits the horizontally polarized (*s*-polarization) component of the beam and reflects the vertically polarized (*p*-polarization) component. The polarization can be altered by rotating the half-wave plate, allowing the power split into the local oscillator leg to be continuously adjusted so as to ensure local oscillator shot-noise-limited detection.

The power split into the local oscillator leg is then frequency shifted 200 MHz by an acousto-optic modulator (AOM). The AOM is an IntraAction Corporation model AQS-2002A1, which has a diffraction efficiency of 20% into the first order. The zero-order beam is stopped by a beam dump to prevent backscatter.

The portion of the beam not split into the local oscillator leg passes through a "transmit-receive" switch, consisting of the combination of a polarizing beamsplitter cube and an Electro Optics Technology model 1845-5 Faraday optical rotator. The light transmitted by the first beamsplitter is horizontally polarized, so it is transmitted through the second beamsplitter as well. The optical rotator rotates the polarization by 45 deg, and the beam then travels to a target. The return from the target then passes through the optical rotator, rotating the polarization an additional 45 deg. When the return encounters the beamsplitter, the beam is vertically polarized and is thus reflected into the signal leg. Note that the target used does not affect the analysis, because our analysis begins at the point where power is coupled into the fibers. However, several targets have been used, including mirrors and a flame-sprayed aluminum diffuse target.

The return signal and the frequency shifted local oscillator are then coupled into a Canadian Instrumentation model 905P-TC-HR variable ratio, single-mode, polarization-preserving evanescent wave coupler. This evanescent wave coupler is used to mix the local oscillator and the return signal into a single fiber pigtailed to the heterodyne detector. The fibers in the evanescent wave coupler are standard single-mode, polarization-preserving fibers with elliptical cores. Using free-space single-mode fiber couplers, the return signal and local oscillator are each coupled into one of the single-mode fibers. For the best mixing efficiency, the polarization of the two beams must be matched, so before coupling the beams into the fibers, half-wave plates are used to align the polarization.

The system can be easily configured for direct detection, as shown in Fig. 2. The first half-wave plate is adjusted so that none of the laser power is reflected into the local oscillator leg. Because the photodetector we chose to use is ac coupled, a Laser Precision model CTX-534 chopper operating at 2 kHz is then added to modulate the beam transmitted to the target. The beam then passes through the transmit receive switch as before, encounters the target and is reflected into the return signal leg. The return is in turn coupled into a small section of single-mode fiber, which is connected with ST-type connectors to an Optics for Research free-space fiber-to-fiber coupler. A 4-nm optical bandpass filter centered at 1.064 μm is placed in this fiber-to-fiber coupler to filter out excess background noise. The signal is then coupled to the fiber pigtailed to the detector to generate the direct detection signal.

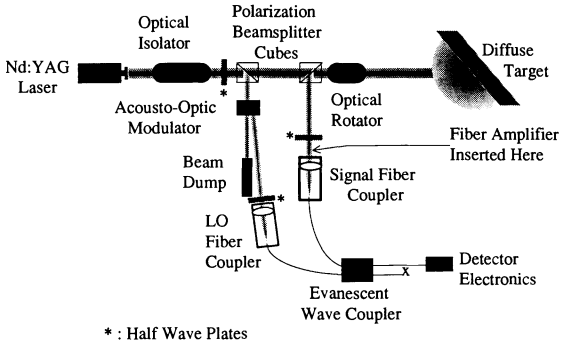

Fig. 1 Heterodyne detection ladar system. The 1.064-μm ladar is shown in its heterodyne configuration. The insertion point of the fiber amplifier into the return signal leg is shown. The detection electronics are shown in detail in Fig. 5.

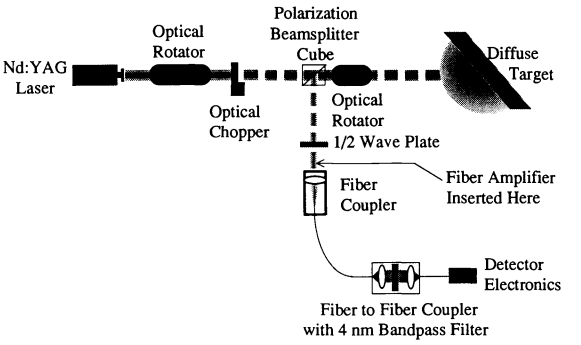

Fig. 2 Direct detection ladar system. The 1.064-μm ladar is shown in its direct detection configuration. There is no optical power split into the local oscillator leg, and an optical chopper has been added to modulate the beam. The insertion point of the fiber amplifier into the return signal leg is shown. The detection electronics are given in detail in Fig. 5.

3 Fiber Amplifier Design

Note that both Figs. 1 and 2 indicate the location at which the optical fiber amplifier is to be added to the respective ladar systems. This section describes the doped fiber used for the amplifier and gives the design for incorporating the amplifier into the ladar system. The amplifier is designed so the return signal and the pump light are coupled into the fiber simultaneously.

A 25-m spool of doped fiber was obtained from Rutgers University. This fiber has an unusual profile, as shown in Fig. 3. The fiber has a nearly rectangular inner cladding, used to couple laser diode pump light into the fiber. The single-mode core is doped with the rare-earth ion Nd^{3+} and codoped with aluminum.

Figure 4 shows the setup used to couple the return signal and the pump light into the fiber amplifier.[6] The laser diode used to pump the fiber is a Laser Diode Incorporated model LDT 26010 laser diode with an 808.4-nm, 500-mW cw output. A built-in thermoelectric (TE) cooler acts as a heat pump to cool the laser diode emitter. As the laser diode is cooled, its output wavelength decreases, allowing the wavelength to be tuned over a small range. The peak absorption wavelength of the neodymium-doped fiber obtained from Rutgers University was given to be 805 nm. Using the TE cooler, the wavelength of the laser diode is then shifted to the peak absorption of the fiber.

A thermistor monitors the temperature of the diode, with a feedback loop varying the current to the TE cooler to maintain a constant thermistor value. This gives the diode a stable output in both power and wavelength to keep the operating conditions of the fiber amplifier constant.

A graded-refractive-index (GRIN) rod lens from a Newport F-GRK1 graded-index rod lens kit is used to minimize the divergence of the beam from the laser diode. A dichroic mirror transmits the 1.064-μm return signal and reflects the 805-nm pump light. This allows the signal and the pump to be coupled into the fiber simultaneously using a Newport F-1015 high-precision single-mode fiber coupler. The fiber amplifier is then inserted into the return signal leg, with the output end of the fiber connectorized with an AT&T ST-type connector. The amplified signal is coupled via this connector into the fibers leading to the bandpass filter unit, which blocks excess background light (of primary concern during direct detection) and any unabsorbed pump light. The amplified signal is then launched into the signal arm of the evanescent wave coupler, during heterodyne detection, or is used to directly illuminate the photodetector during direct detection.

4 SNR Theory for Direct Detection

The SNR is defined to be the ratio of the signal power to the noise power. This section provides a theoretical analysis of the overall postdetection electronic SNR for the ladar test bed in a direct detection configuration, considering detection both with and without the fiber amplifier. The analysis begins with a discussion of the optical power incident on the detector and follows with a derivation of the signal and noise voltages after the detection electronics.

4.1 *Direct Detection Without the Fiber Amplifier*

For a direct detection scheme, the outgoing continuous wave laser power must be modulated so the signal current can be ac coupled into the postdetection electronics. The optical chopper modulating the beam gives a 2-kHz square-wave return signal. Figure 5 shows the electronic scheme between the detector and the spectrum analyzer used to measure the SNR. The detector is a Lasertron QDFT-250-301 *p-i-n* field effect transistor (FET) detector package, with a multimode fiber pigtail. The photodetector is saturated at 220 μW of power and has a bandwidth of 250 MHz. The package includes an integrated current-to-voltage preamplifier with a transimpedance of 5.9 kΩ. The detector package is terminated with a 975-Ω load as a precautionary measure, as recommended by the manufacturer, and is then ac coupled to an electronic amplifier. For direct detection, the electronic amplifier is an Analog Modules 324A-3-B voltage amplifier with an input impedance of $R_{amp} = R_a = 1$ MΩ, a voltage gain $g = g_a = 1000$, and an amplification bandwidth from 200 Hz to 35 MHz. The amplified voltage is then connected to the 50-Ω input of a Tektronix 495P spectrum analyzer whose resolution bandwidth has been set to 10 Hz.

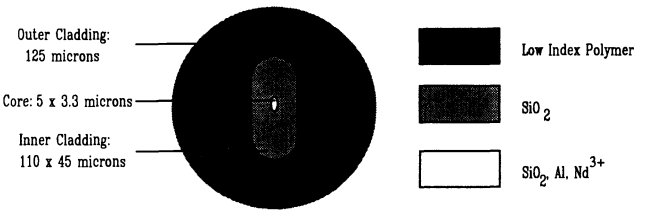

Fig. 3 Geometry of the Rutgers neodymium-doped fiber. The unusual aspect of the fiber is the rectangular inner cladding, used to couple the pump light from the laser diode into the fiber.

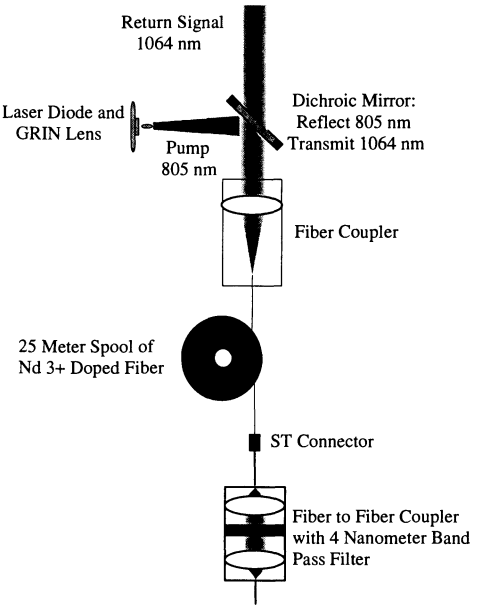

Fig. 4 Fiber amplifier pump scheme. A dichroic mirror is used to couple the pump light and the return signal light into the doped fiber. The pump is a laser diode operating at 805 nm, with a graded-refractive-index (GRIN) lens used to minimize the divergence. After the fiber amplifier a 4-nm bandpass filter is inserted to block excess pump light and minimize the spontaneous emission. After the bandpass filter, the output is connected to the evanescent wave coupler for heterodyne detection (see Fig. 1) and directly to the detector for direct detection (see Fig. 2).

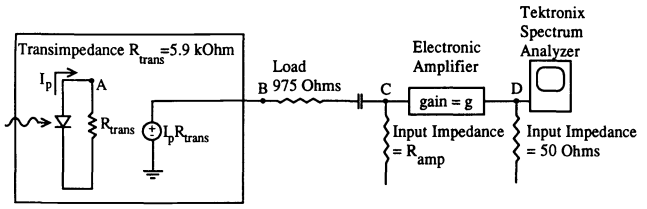

Fig. 5 Detection electronics. The Lasertron detector package includes the photodetector and a current-to-voltage amplifier. A safety load of 975 Ω is used to terminate the detector package. An electronic amplifier is used to boost the voltage into the spectrum analyzer used to measure the SNR.

The signal current from the detector, i_r, at node A in Fig. 5 is given by

$$i_r = \Re P_r[\mathrm{sqr}(2\pi ft)] \ , \tag{1}$$

where $\Re = 0.704$ A/W is the responsivity of the detector package, P_r is the optical return signal power, and the square-wave function (sqr) in Eq. (1) represents a 50% duty cycle positive square-wave function (i.e., values of only zero and one). The signal voltage V_r just after the integrated preamplifier (at node B in Fig. 5) is then

$$V_r = i_r R_{\mathrm{trans}} = \Re P_r R_{\mathrm{trans}}[\mathrm{sqr}(2\pi ft)] \ , \tag{2}$$

where $R_{\mathrm{trans}} = 5.9$ kΩ is the transimpedance of the preamplifier. The voltage is then amplified by the Analog Modules amplifier to yield a voltage at node D of

$$V_{r,\mathrm{amp}} = g_a V_r = g_a \Re P_r R_{\mathrm{trans}}[\mathrm{sqr}(2\pi ft)] \ , \tag{3}$$

where we note that because of the large input impedance of the Analog Modules amplifier, there is no appreciable voltage drop across the 975-Ω series resistance. The signal power, Γ_{r1}, seen by the spectrum analyzer centered at 2 kHz, is then

$$\Gamma_{r1} = \frac{\langle V_{r,\mathrm{amp}}^2 \rangle}{R_{\mathrm{SA}}} = \frac{(g_a \Re P_r R_{\mathrm{trans}})^2 (1/2)}{R_{\mathrm{SA}}} \ , \tag{4}$$

where $R_{\mathrm{SA}} = 50$ Ω is the input impedance of the spectrum analyzer.

The total noise from the detector consists of shot noise from the optical return signal power on the detector, dark current noise, and thermal noise. The well-known equations for these noise components, given as mean-squared noise currents, are $\langle i_q^2 \rangle = 2eB_e\langle i_r \rangle$, $\langle i_d^2 \rangle = 2eB_e I_d$, and $\langle i_t^2 \rangle = 4kB_eT/R_{\mathrm{trans}}$, respectively, where e is the charge on an electron, B_e is the electronic bandwidth of the detector, I_d is the detector dark current, k is the Boltzmann constant, T is the temperature in degrees Kelvin, and $\langle i_r \rangle = \Re P_r/2$ is the average signal current from Eq. (1) (Ref. 7 and see, e.g., Refs. 8 and 9).

The total mean-squared detector noise $\langle i_n^2 \rangle$ is then

$$\langle i_n^2 \rangle = \langle i_q^2 \rangle + \langle i_d^2 \rangle + \langle i_t^2 \rangle = 2eB_e \Re\left(\frac{P_r}{2}\right) + 2eB_e I_d + \frac{4kB_eT}{R_{\mathrm{trans}}} \ , \tag{5}$$

thus yielding an average detector noise current at node A of[7]

$$\langle i_n^2 \rangle^{1/2} = (\langle i_q^2 \rangle + \langle i_d^2 \rangle + \langle i_t^2 \rangle)^{1/2} = \left(eB_e \Re P_r + 2eB_e I_d + \frac{4kB_eT}{R_{\mathrm{trans}}} \right)^{1/2} \ . \tag{6}$$

Calculating the amplified voltage $V_{n,\mathrm{amp}}$ at node D,

$$V_{n,\mathrm{amp}} = g_a R_{\mathrm{trans}} \langle i_n^2 \rangle^{1/2} = g_a R_{\mathrm{trans}} \left(eB_e \Re P_r + 2eB_e I_d + \frac{4kB_eT}{R_{\mathrm{trans}}} \right)^{1/2} \ . \tag{7}$$

The electrical noise power seen by the spectrum analyzer is thus

$$\Gamma_n = \frac{V_{n,\mathrm{amp}}^2}{R_{\mathrm{SA}}} = \frac{\{g_a R_{\mathrm{trans}}[eB_e \Re P_r + 2eB_e I_d + (4kB_eT/R_{\mathrm{trans}})]^{1/2}\}^2}{R_{\mathrm{SA}}} \ . \tag{8}$$

Note, however, that the noise power terms used in deriving Eq. (8) are white noises in nature, so the power is equally spread across the full electrical bandwidth B_e. The spectrum analyzer thus displays the noise power of Eq. (8) as equally divided among the bandwidth intervals defined by the resolution bandwidth, $\delta\nu = 10$ Hz. The actual noise power level displayed by the spectrum analyzer, $\Gamma_{n,\delta\nu}$, is then obtained by replacing B_e with $\delta\nu$ in Eq. (8), yielding

$$\Gamma_{n,\delta\nu} = \frac{(g_a R_{\mathrm{trans}})^2 \{e(\delta\nu)\Re P_r + 2e(\delta\nu) I_d + [4k(\delta\nu)T/R_{\mathrm{trans}}]\}}{R_{\mathrm{SA}}} \ . \tag{9}$$

This noise power, however, is the noise due to the detector noises alone, and does not include excess noise added by the Analog Modules amplifier. This noise was measured by disconnecting the detector package from the amplifier and measuring the noise level Γ_{amp} on the spectrum analyzer due to the amplifier alone. The total noise power Γ_{N1} is then found by adding this measured value, $\Gamma_{\mathrm{amp}} = -57$ dBm (2 nW), to the noise in Eq. (9), giving

$$\Gamma_{N1} = \Gamma_{n,\delta\nu} + \Gamma_{\mathrm{amp}} = \frac{(g_a R_{\mathrm{trans}})^2 \{e(\delta\nu)\Re P_r + 2e(\delta\nu) I_d + [4k(\delta\nu)T/R_{\mathrm{trans}}]\}}{R_{\mathrm{SA}}} + 2.0 \times 10^{-9} \ \mathrm{W} \ . \tag{10}$$

Using Eqs. (4) and (10), the direct detection SNR equation without the fiber amplifier in place is

$$\mathrm{SNR}=\frac{\Gamma_{r1}}{\Gamma_{N1}}$$

$$=\frac{(1/2)(g_a\Re P_r R_{\mathrm{trans}})^2}{(g_a R_{\mathrm{trans}})^2\{e(\delta\nu)\Re P_r+2e(\delta\nu)I_d+[4k(\delta\nu)T/R_{\mathrm{trans}}]\}+R_{\mathrm{SA}}\cdot 2.0\times 10^{-9}\ \mathrm{W}} \quad (11)$$

A useful measure of detection sensitivity can be obtained by plotting the SNR from Eq. (11) as a function of the return signal power P_r, as shown in Fig. 6. A summary of the variables used in Eq. (11) is given in Sec. 8. The plot can be used to determine the return power necessary to achieve a specified threshold SNR, defined to be the minimum SNR at which a return signal can be reliably discerned from the noise. The threshold SNR has been chosen to give a high probability of detection for normal values of the probability of false alarm.[10] From Fig. 6, the minimum detectable return signal for direct detection without the fiber amplifier for our chosen threshold SNR of 6 is 0.263 nW. This will be compared to the value for direct detection with the fiber amplifier, derived in the following subsection.

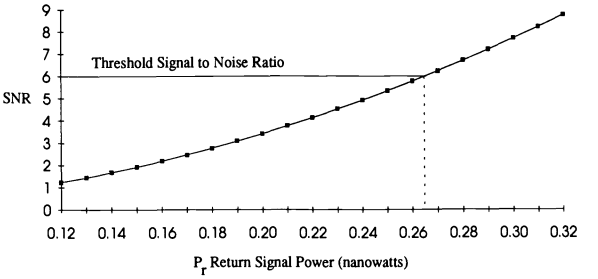

Fig. 6 Direct detection SNR versus return signal power. The SNR as a function of return signal power for direct detection without the fiber amplifier is shown [see Eq. (11)]. The threshold SNR of 6 is defined to be the SNR required to discern a signal above the noise. A return signal power of 0.263 nW is required to reach the threshold SNR.

4.2 *Direct Detection with the Fiber Amplifier*

For direct detection with the fiber amplifier, the return signal is increased by a power gain factor G. This gain factor depends on the amount of pump light absorbed and the length of the fiber. With our 500-mW laser diode pump, measured gains of 1 dB/m have been achieved. With 25 m of fiber, the gain of 25 dB corresponds to a power gain factor of $G=316$. The electrical signal power shown by the spectrum analyzer, given by Eq. (4) for direct detection without the amplifier, thus becomes

$$\Gamma_{r2}=\frac{(1/2)(g_a\Re G P_r R_{\mathrm{trans}})^2}{R_{\mathrm{SA}}} \quad . \quad (12)$$

The detector and electronic amplifier noises previously discussed do not change, with the exception of the shot-noise term. The shot noise is increased because the signal power is amplified by G and because there are spontaneous emission photons from the fiber amplifier directly adding to the shot-noise term. Modifying Eq. (10) accordingly, the detector noise plus electronic amplifier noise now becomes

$$\Gamma_{N2}=\frac{(g_a R_{\mathrm{trans}})^2\{2e(\delta\nu)\Re[G(P_r/2)+P_{\mathrm{se}}]+2e(\delta\nu)I_d+[4k(\delta\nu)T/R_{\mathrm{trans}}]\}}{R_{\mathrm{SA}}}+2.0\times 10^{-9}\ \mathrm{W}\ , \quad (13)$$

where P_{se} is the average spontaneous emission power incident on the detector.

In general, the average spontaneous emission power is dependent on the number of free-space modes considered. For a single-mode fiber amplifier, the spontaneous emission power propagating through the fiber is limited to the fraction of photons emitted by the dopant into the single propagating mode of the fiber, and is given by[11]

$$P_{\mathrm{se}}=Gh\nu B_o \ , \quad (14)$$

where h is Planck's constant, ν is the optical frequency of the return signal, and B_o is the optical bandwidth of the spontaneous emission. The 4-nm bandpass filter, centered at the optical frequency of the return signal, defines this bandwidth such that $B_o=1.07\times 10^{12}$ Hz. For reasons similar to those discussed prior to Eq. (9), the optical bandwidth of the spontaneous emission is broken into small frequency intervals, the smallest measurable frequency increment being the resolution bandwidth of the spectrum analyzer. The power in a single frequency component is thus obtained by replacing B_o in Eq. (14) with the spectrum analyzer resolution bandwidth $\delta\nu$ to yield

$$P_{\mathrm{se},\delta\nu}=Gh\nu\delta\nu \ . \quad (15)$$

In addition to the increased shot noise in Eq. (13), there are two noise terms arising as a result of spontaneous emission. The first of these terms arises because of beating between the spontaneous emission and the return signal, whereas the second arises because of the spontaneous emission beating with itself, both of which result from the square-law detection of optical radiation.[12]

The spontaneous emission-return signal beat noise occurs when a spontaneous emission component beats with the return signal. This noise is manifest at a frequency equal to the separation between the center frequency of the return signal and the frequency of the spontaneous emission noise components. The spontaneous emission–spontaneous emission beat noise occurs between two spontaneous emission components of different frequencies. A detailed analysis of the beat noises caused by spontaneous emission can be found in Appendix A of Ref. 12.

Only the portion of the spontaneous emission–return signal beat noise contributing to the SNR at the signal modulation frequency must be considered. This portion of the beat noise occurs when spontaneous emission components separated by $+/-2$ kHz from the optical frequency of the return signal beat with the return signal. The electric field incident on the detector from the return signal and these two spontaneous emission components is[12]

$$\mathbf{E} = \sqrt{GP_r}\cos(\omega_o t)\hat{a}_r + (2P_{\mathrm{se},\delta\nu})^{1/2} \times \{\cos[(\omega_o - 2\pi f)t + \Phi_{-f}]\hat{b}_{-f} + \cos[(\omega_o + 2\pi f)t + \Phi_{+f}]\hat{b}_{+f}\} \ , \quad (16)$$

where $f = 2$ kHz is the signal modulation frequency, Φ_f and Φ_{-f} are the random phases for the respective spontaneous emission components, $P_{\mathrm{se},\delta\nu}$ is the spontaneous emission power in one 10-Hz frequency component, $\hat{a}_r$ is the linear polarization of the return signal, $\hat{b}_{-f}$ and $\hat{b}_{+f}$ are the random polarizations of the two spontaneous emission components, and $\omega_o = 2\pi \cdot 2.82 \times 10^{14}$ is the angular frequency of the return signal. Recall now that the detector current resulting from an electric field is equal to the responsivity of the detector multiplied by the magnitude squared of the electric field vectors such that

$$i = \Re|\mathbf{E}|^2 \ . \quad (17)$$

When Eq. (16) is substituted into Eq. (17), two 2-kHz beat noise current terms arise from the beating between the spontaneous emission and the return signal. These terms are manipulated using trigonometric identities, resulting in the return signal–spontaneous emission beat noise current:

$$i_{r-\mathrm{se},2\mathrm{kHz}} = \Re(2GP_rP_{\mathrm{se},\delta\nu})^{1/2}[\cos(2\pi ft + \Phi_{-f})\Psi_{-f} + \cos(-2\pi ft + \Phi_f)\Psi_f] \ , \quad (18)$$

where Ψ_{-f} and Ψ_f are random efficiency terms (i.e., $0 \leq \Psi_{\pm f} \leq 1$) arising because of the polarization mixing of the two fields.

As for the spontaneous emission–spontaneous emission beat noise, the electric fields resulting from all spontaneous emission components must be considered, with any pair of components separated by 2 kHz contributing to the SNR noise terms at 2 kHz. The spontaneous emission electric field is represented by a summation of components,[12] each of which is separated by the resolution bandwidth of the spectrum analyzer, $\delta\nu = 10$ Hz, from its nearest neighboring frequency component. That is,

$$\mathbf{E}_{\mathrm{se}} = \sum_{k=-M}^{M} (2P_{\mathrm{se},\delta\nu})^{1/2}\cos[(\omega_o + 2\pi k\delta\nu)t + \Phi_k]\hat{b}_k \ , \quad (19)$$

where $-M$ and M designate spontaneous emission frequency components at the edges of the 4-nm ($B_o = 1.07 \times 10^{12}$ Hz) bandpass filter. To arrive at the corresponding noise current, the magnitude squared of $\mathbf{E}_{\mathrm{se}}$ is multiplied by the responsivity of the detector. When the summation of Eq. (19) is squared, the cross terms give rise to the spontaneous emission–spontaneous emission beat noise current, although we consider only those beat terms affecting the SNR at 2 kHz. This current is then written as a summation of those terms beating at 2 kHz, to yield

$$i_{\mathrm{se}-\mathrm{se},2\mathrm{kHz}} = \Re 2P_{\mathrm{se},\delta\nu}\sum_{j=1}^{N}[\cos(2\pi ft + \Phi_j)\Psi_j] \ , \quad (20)$$

where Φ_j is the random phase of each beat component, Ψ_j is a term that takes into account the polarization mixing efficiency, and N is the number of spontaneous emission beat terms at 2 kHz. The optical bandwidth, $B_o = 1.07 \times 10^{12}$ Hz, contains 1.07×10^{11} of the 10-Hz frequency increments, and there are 200 frequency increments in the 2-kHz band. The total number of components separated by 2 kHz, and thus the number beating at that frequency, is obtained by $N = 1.07 \times 10^{11} - 200 \approx 1.07 \times 10^{11}$.

The beat-noise currents given by Eqs. (18) and (20) are then analyzed through the transimpedance amplifier, the electronic amplifier, and the spectrum analyzer, resulting in

$$\Gamma_{n,r-\mathrm{se}} = \frac{\langle (g_a R_{\mathrm{trans}} i_{r-\mathrm{se},2\mathrm{kHz}})^2 \rangle}{R_{\mathrm{SA}}} = \frac{(g_a R_{\mathrm{trans}}\Re)^2}{R_{\mathrm{SA}}} GP_rP_{\mathrm{se},\delta\nu} \quad (21)$$

and

$$\Gamma_{n,\mathrm{se}-\mathrm{se}} = \frac{\langle (g_a R_{\mathrm{trans}} i_{\mathrm{se}-\mathrm{se},2\mathrm{kHz}})^2 \rangle}{R_{\mathrm{SA}}} = \frac{(g_a R_{\mathrm{trans}}\Re P_{\mathrm{se},\delta\nu})^2}{R_{\mathrm{SA}}} N \quad (22)$$

for the return signal–spontaneous emission and spontaneous emission–spontaneous emission beat noise power terms, respectively.

Adding the beat-noise terms from Eqs. (21) and (22) to the detector noises from Eq. (13) and including the signal power from Eq. (12), the $\mathrm{SNR}_{\mathrm{dir},w}$ for direct detection with the fiber amplifier is

$$\mathrm{SNR}_{\mathrm{dir},w} = \frac{\Gamma_{r2}}{\Gamma_{N2} + \Gamma_{r-\mathrm{se}} + \Gamma_{\mathrm{se}-\mathrm{se}}} = \frac{(1/2)(g_a\Re GP_rR_{\mathrm{trans}})^2}{(g_aR_{\mathrm{trans}})^2\Lambda_n + R_{\mathrm{SA}} \cdot 2.0 \times 10^{-9}\ \mathrm{W}} \ , \quad (23)$$

where

$$\Lambda_n = 2e(\delta\nu)\Re\left[G\left(\frac{P_r}{2}\right) + P_{\mathrm{se}}\right] + 2e(\delta\nu)I_d + \frac{4k(\delta\nu)T}{R_{\mathrm{trans}}} + \Re^2 GP_rP_{\mathrm{se},\delta\nu} + (\Re P_{\mathrm{se},\delta\nu})^2 N \ . \quad (24)$$

Figure 7, a plot of SNR versus return signal power for Eq. (23), shows that the signal required to reach the threshold SNR of 6 is 2.28 pW. The values used to plot Eq. (23) are found in Sec. 8. This value is 20.6 dB smaller than the power

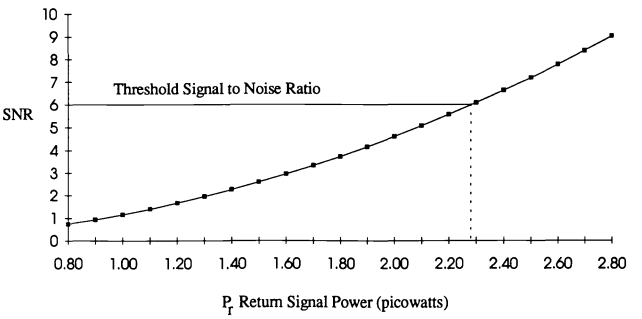

Fig. 7 Direct detection SNR versus return signal power with the fiber amplifier. Equation (23) was used to plot the SNR as a function of return signal power for direct detection with the fiber amplifier. A return signal power of 2.28 pW is required to reach the threshold SNR.

required to reach the threshold for direct detection without the fiber amplifier, thus showing a significant increase in sensitivity obtained by adding the fiber amplifier to the direct detection system.

5 SNR Analysis for Heterodyne Detection

This section provides a theoretical analysis of the SNR for heterodyne detection, both with and without the fiber preamplifier included. As we will show, an additional noise term must be accounted for because of beating effects between the local oscillator and spontaneous emission fields. As a result of this new noise term, the sensitivity gains when using the fiber preamplifier in a heterodyne ladar system are not as dramatic as those achieved for the direct detection case.

5.1 *Heterodyne Detection Without the Fiber Amplifier*

The detection electronics are again given in Fig. 5. The detector package is the same as used for direct detection, but a higher frequency electronic amplifier must be used to ensure amplification of the 200 MHz IF signal. Our choice of amplifiers has been a Miteq AU-4A-0150 amplifier, with a 50-Ω input impedance, a power gain of 61 dB, and an amplification bandwidth from 1 to 500 MHz.

Recall, in a heterodyne detection scheme, a local oscillator is mixed with the return signal to improve receiver sensitivity. For the test system being considered, the local oscillator is frequency shifted by an amount $\Delta = 200$ MHz. Referring back to Fig. 1, the local oscillator and return signal mix at the photodetector, resulting in two dc current terms and one beat term oscillating at the 200-MHz IF. Without the fiber amplifier in place, the IF current term i_{IF}, is written as

$$i_{\mathrm{IF}} = \Re[2(P_r P_{\mathrm{LO}})^{1/2} \cos(2\pi \Delta t)] \ . \tag{25}$$

After the integrated current-to-voltage preamplifier, the IF signal at node B of Fig. 5 becomes

$$V_{\mathrm{IF}} = i_{\mathrm{IF}} R_{\mathrm{trans}} = 2\Re R_{\mathrm{trans}} (P_r P_{\mathrm{LO}})^{1/2} \cos(2\pi \Delta t) \ . \tag{26}$$

For this detection scheme, the input impedance of the Miteq amplifier is not large enough to neglect voltage division with respect to the 975-Ω safety load resistance. The actual voltage seen by the amplifier at node C is thus reduced by a factor D, given as

$$D = \frac{50\ \Omega}{975\ \Omega + 50\ \Omega} = 0.048 \ . \tag{27}$$

The gain from the Miteq amplifier is a power gain of 61 dB, corresponding to a voltage gain of $g = g_m = 1122$. The voltage after the amplifier, $V_{\mathrm{IF,amp}}$ at node D, is thus

$$\begin{aligned} V_{\mathrm{IF,amp}} &= g_m D V_{\mathrm{IF}} \\ &= 2 g_m D \Re R_{\mathrm{trans}} (P_r P_{\mathrm{LO}})^{1/2} \cos(2\pi \Delta t) \ , \end{aligned} \tag{28}$$

whereas the spectrum analyzer sees the following power level, $\Gamma_{\mathrm{IF}a}$, centered at 200 MHz:

$$\Gamma_{\mathrm{IF}a} = \frac{\langle V_{\mathrm{IF,amp}}^2 \rangle}{R_{\mathrm{SA}}} = \frac{2(g_m D \Re R_{\mathrm{trans}})^2 P_r P_{\mathrm{LO}}}{R_{\mathrm{SA}}} \ . \tag{29}$$

The derivation for the noise power level for the heterodyne detection case without the fiber amplifier is very similar to the derivation used to obtain Eq. (10). The noise power level for heterodyne detection without the amplifier, Γ_{N3}, is then

$$\begin{aligned} \Gamma_{N3} = &\frac{(g_m D R_{\mathrm{trans}})^2 \{2e(\delta\nu)\Re(P_r + P_{\mathrm{LO}}) \\ &+ 2e(\delta\nu) I_d + [4k(\delta\nu)T/R_{\mathrm{trans}}]\}}{R_{\mathrm{SA}}} \\ &+ 6.3 \times 10^{-14}\ \mathrm{W} \ , \end{aligned} \tag{30}$$

where the electronic amplifier noise, measured for the Miteq amplifier by the same method as for the Analog Modules amplifier, was determined to be 6.3×10^{-14} W. In comparison to Eq. (10), a shot-noise term resulting from local oscillator power P_{LO} has been added, and a factor of 2 multiplying the total shot-noise term has been included, as the outgoing signal is no longer chopped [see Eqs. (4) and (5)]. Also, the voltage divider effect D has been included.

For the heterodyne detection case without the fiber amplifier, it is convenient to note the limiting noises of the detection scheme. With a measured local oscillator power of 200 μW, the various noise terms can be evaluated to show that the local oscillator shot noise dominates the other noise factors by almost 10 dB, thus ensuring local oscillator shot-noise-limited detection. The noise power, under this limiting case, then becomes

$$\Gamma_{N3} = \frac{(g_m D R_{\mathrm{trans}})^2 2e(\delta\nu)\Re(P_{\mathrm{LO}})}{R_{\mathrm{SA}}} \ . \tag{31}$$

Taking the ratio of Eqs. (30) and (31) yields the signal-to-noise ratio, $\mathrm{SNR}_{\mathrm{het},w/o}$, for heterodyne detection without the fiber amplifier, given as

$$\mathrm{SNR}_{\mathrm{het},w/o} = \frac{\Gamma_{\mathrm{IF}a}}{\Gamma_{N3}} = \frac{2(g_m D \Re R_{\mathrm{trans}})^2 P_r P_{\mathrm{LO}}}{(g_m D R_{\mathrm{trans}})^2 2e(\delta\nu)\Re(P_{\mathrm{LO}})} \ . \tag{32}$$

Figure 8 is the plot of SNR versus return signal power from Eq. (32) using parameters found in Sec. 8. We see from this figure that 1.54×10^{-17} W of return signal power are required to reach the SNR threshold of 6.

5.2 *Heterodyne Detection with the Fiber Amplifier*

For heterodyne detection with the fiber amplifier in place, the return signal is increased by the power gain factor G. The total electric field incident on the detector is composed of the amplified return signal, the local oscillator, and the spontaneous emission.

The IF signal power, given by Eq. (29) for heterodyne detection without the fiber amplifier, becomes

$$\Gamma_{\mathrm{IF}b} = \frac{2(g_m D \Re R_{\mathrm{trans}})^2 G P_r P_{\mathrm{LO}}}{R_{\mathrm{SA}}} \ . \tag{33}$$

The detector and electronic noise power level for detection with the fiber amplifier is similar to Eq. (30). However, the return signal power is increased by G in the heterodyne shot-noise term, and the spontaneous emission power adds another

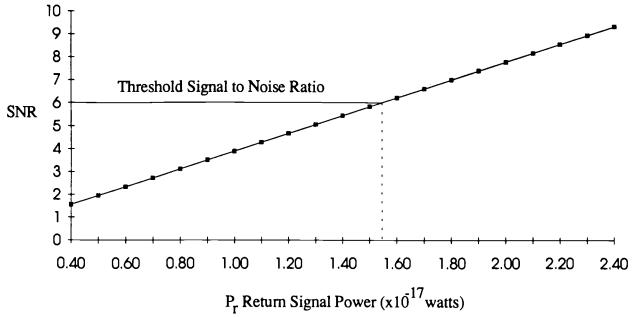

Fig. 8 Heterodyne detection SNR versus return signal power. The plot shows the SNR as a function of return signal power for heterodyne detection, without the fiber amplifier, using Eq. (32). A return signal power of 1.54×10^{-17} W is required to reach the threshold SNR.

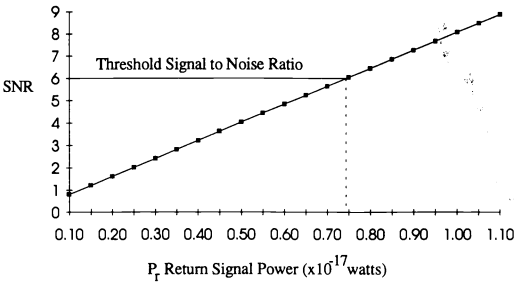

Fig. 9 Heterodyne detection SNR versus return signal power with the fiber amplifier. Equation (36) was used to plot the SNR as a function of return signal power for direct detection with the fiber amplifier. A return signal power of 7.45×10^{-18} W is required to reach the threshold SNR.

component to the shot-noise term. The electronic and detector noise power level is thus

$$\Gamma_{N4}=\frac{(g_m D R_{\text{trans}})^2\{2e(\delta\nu)\Re(GP_r+P_{\text{LO}}+P_{\text{se}})+2e(\delta\nu)I_d+[4k(\delta\nu)T/R_{\text{trans}}]\}}{R_{\text{SA}}}+6.3\times10^{-14}\ \text{W}\ . \tag{34}$$

For the heterodyne case, three spontaneous emission beat-noise terms must be added to Eq. (34). The first two terms are the spontaneous emission–return signal beat noise and the spontaneous emission–spontaneous emission beat noise. These noise terms are the same as for the direct detection case and are described in Eqs. (21) and (22). The third term results from the beating between the spontaneous emission and the local oscillator and has the same form as the spontaneous emission–return signal beat noise term, given by Eq. (21). The spontaneous emission–local oscillator beat noise term is obtained by replacing the amplified return signal power, GP_r, in this equation with the local oscillator power, P_{LO}. The beat noises are thus given as[12]

$$\Gamma_{n,\text{beat}}=\Gamma_{n,\text{se}-r}+\Gamma_{n,\text{se}-\text{LO}}+\Gamma_{n,\text{se}-\text{se}}=\frac{(\Re g_m D R_{\text{trans}})^2}{R_{\text{SA}}}(GP_r P_{\text{se},\delta\nu}+P_{\text{LO}}P_{\text{se},\delta\nu}+P^2_{\text{se},\delta\nu}N_h)\ . \tag{35}$$

It is important to note that N_h in Eq. (35) represents the number of beat-noise terms at 200 MHz. Again, there are 1.07×10^{11} incremental frequency components in B_o and 2.00×10^{7} of the components in the 200-MHz band. The total number of terms beating at 200 MHz is obtained by $N=1.07\times10^{11}-2.00\times10^{7}\approx1.07\times10^{11}$. The SNR for heterodyne detection with the fiber amplifier is obtained from Eqs. (33), (34), and (35) to yield

$$\text{SNR}_{\text{het},w}=\frac{\Gamma_{\text{IF}b}}{\Gamma_{N4}+\Gamma_{n,\text{beat}}}=\frac{2(g_m D\Re R_{\text{trans}})^2 GP_r P_{\text{LO}}}{(g_m D R_{\text{trans}})^2\Lambda_n+R_{\text{SA}}\cdot6.3\times10^{-14}\ \text{W}}\ , \tag{36}$$

where

$$\Lambda_n=2e(\delta\nu)\Re(GP_r+P_{\text{LO}}+P_{\text{se}})+2e(\delta\nu)I_d+\frac{4k(\delta\nu)T}{R_{\text{trans}}}+G\Re^2P_rP_{\text{se},\delta\nu}+\Re^2P_{\text{LO}}P_{\text{se},\delta\nu}+(\Re P_{\text{se},\delta\nu})^2N_h\ . \tag{37}$$

Figure 9 shows the SNR versus return signal power for heterodyne detection with the fiber amplifier from Eq. (36), using the values found in Sec. 8. We see that the return signal power required to reach the threshold SNR is 7.45×10^{-18} W, giving an increase in the sensitivity of the heterodyne detection system of only 3.1 dB, with the fiber amplifier added. This is because the local oscillator shot noise is no longer the dominating noise. Using the variables in Sec. 8, the noise terms can be examined to show that the beat noises added due to the spontaneous emission dominate the shot noise by 21 dB! This counters the higher IF signal power and gives only a slight increase in SNR for heterodyne detection with the fiber amplifier.

6 Initial Experimental Results

The fiber amplifier setup was assembled as shown in Fig. 5, and initial measurements were made to determine the small signal gain characteristics of the Nd^{3+}-doped fiber amplifier at the return signal wavelength of 1064 nm. Using a dichroic mirror, the laser diode pump and a 1064-nm test signal were coupled into the fiber amplifier. The pump laser diode provides 500 mW of pump power at 805 nm (see Sec. 3), whereas the test signal is supplied by tapping off a small portion of the unmodulated Nd:YAG laser used in the ladar system of Fig. 1.

To measure the signal power P_s coupled into the fiber amplifier, the pump is blocked and the output power is measured after the 4-nm bandpass filter. To then measure the spontaneous emission power P_{se}, the signal is similarly blocked and another measurement is taken after the bandpass filter (note that any excess pump light not absorbed by the dopant is blocked by the filter). Next, both the signal and the pump are coupled into the fiber amplifier in order to measure P_{comb}, the amplified signal power combined with the spontaneous emission power after the filter. The fiber amplifier small signal gain can then be calculated from these three measurements.

Based on these procedures, the following measurements have been made:

$P_s = 1.7\ \mu W$,

$P_{se} = 47.5\ \mu W$,

$P_{comb} = 493\ \mu W$.

Note that in the small signal gain regime, the input signal power is small enough such that after amplification the excited state population is not appreciably depleted. The spontaneous emission power from the fiber amplifier is therefore largely unaffected by the addition of the signal. Separate measurements have indicated that signal powers of the order of several milliwatts are required to significantly depopulate the amplifier excited state such that there are detectable decreases in spontaneous emission power. Because a ladar return signal of 1.7 μW would correspond to a very large return signal (see, for example Figs. 6 to 9), this small signal gain analysis is appropriate for determining the gain of the amplifier for most applications of our ladar system.

The fiber amplifier gain G is then calculated as follows:

$$G = \frac{P_{comb} - P_{se}}{P_s} = 262\ (24.2\ \text{dB}) \ . \tag{38}$$

The measured gain of 24.2 dB corresponds very well with the assumed gain of 25 dB used to generate Figs. 6 to 9. Thus, by incorporating this fiber amplifier into the ladar system, our preceding theoretical SNR analysis can be evaluated experimentally. Currently, the fiber amplifier has been fully incorporated into the ladar system, and preliminary measurements show SNR increases of the order of those predicted. A companion paper will be submitted for publication when conclusive data has been collected and analyzed.

7 Summary

We have derived the SNR for a direct detection and heterodyne detection ladar system for two cases—detection without a fiber amplifier and detection with a fiber amplifier.

The plots of SNR versus return signal power, Figs. 6 and 7, show an increase in sensitivity for the direct detection scheme we have considered. The return signal power required to obtain a threshold SNR for detection with the fiber amplifier is 20.6 dB lower than the power required for the case without the fiber amplifier. These results are, however, very dependent on the postdetection electronics, which define the limiting noises. For a system designed with more sophisticated postdetection electronics, the increase in sensitivity might not be as large when a fiber amplifier is added, because of the lower limiting noises. The primary application of a fiber amplifier is in increasing the sensitivity of a noisy direct detection ladar system. By incorporating a fiber amplifier, trade-offs can be made when designing a system, allowing lighter, less expensive detection electronics to be used without sacrificing sensitivity.

For the heterodyne detection scheme, Figs. 8 and 9 show a small increase of 3.1 dB in sensitivity when the fiber amplifier is added to the system. For heterodyne detection without the fiber amplifier, the local oscillator shot noise dominates the detection process. With the addition of the fiber amplifier, however, the spontaneous emission beat noises dominate the detection process, so the increase in return signal power is directly offset by the increase in noise caused by the spontaneous emission.

Although the sensitivity of a direct detection ladar system is increased with the addition of a fiber amplifier, it is important to note that the direct detection performance is still less than the performance of the heterodyne system. The direct detection system is significantly simpler, however, and an increase in sensitivity warrants an examination of the trade-offs between the performance and the simplicity of the detection scheme.

Experimentally, a neodymium-doped fiber was configured into a fiber amplifier with a measured gain of 24.2 dB. The fiber amplifier has been fully incorporated into a 1-μm ladar system, and initial experimental data show SNR increases of the order of those predicted in the analysis. The incorporation of optical fiber amplifiers thus shows promise for application in the next generation of ladar receiver technology.

8 Nomenclature

Summary of the variables, and their values, used in the final SNR equations.

B_e	Electrical bandwidth of the detector	250 MHz
B_o	Optical bandwidth of the spontaneous emission (4-nm bandpass filter)	1.07×10^{12} Hz
ν	Optical power center frequency (1.064 μm)	2.82×10^{14} Hz
$\delta\nu$	Spectrum analyzer resolution bandwidth	10 Hz
h	Planck's constant	6.626×10^{-34} J s
G	Fiber amplifier power gain (1 dB/m, 25 m)	316
P_{LO}	Local oscillator power (near detector saturation)	200 μW
P_{se}	Spontaneous emission power, $Gh\nu B_o$	63 μW
$P_{se,\delta\nu}$	Incremental spontaneous emission power, $Gh\nu\delta\nu$	5.9×10^{-16} Hz
g_a	Analog Modules amplifier (direct detection) voltage gain	1000
g_m	Miteq amplifier (heterodyne detection) voltage gain	1122
D	Voltage divider effect Direct detection Heterodyne detection	 1 0.048
R_a	Input impedance of the Analog Modules amplifier	1 MΩ
R_m	Input impedance of the Miteq amplifier	50 Ω
R_{trans}	Transimpedance of the integrated amplifier	5900 Ω
R_{SA}	Spectrum analyzer input impedance	50 Ω
$\Re$	Responsivity of the detector (Lasertron detector)	0.704 A/W
e	Charge of an electron	1.6×10^{-19} C

I_d	Detector dark current (Lasertron detector)	2.9 nA
k	Boltzmann constant	1.38×10^{-23} J/K
T	Temperature	298 K
N	Number of spontaneous emission beat components at 2 kHz (direct detection)	1.07×10^{11}
N_h	Number of spontaneous emission beat components at 200 MHz (heterodyne detection)	1.07×10^{11}

Acknowledgments

Helpful discussions with Edward Watson, Scott McCracken, Jay Overbeck, and Martin B. Mark of the Wright Laboratory Electro-Optic Techniques group are gratefully acknowledged. Special thanks also to Mohammad A. Karim and the University of Dayton Research Council for their continuing support of the authors' research and scholarly activities.

This work has been sponsored by the Wright Laboratory Avionics Directorate and Technology/Scientific Services, Inc., of Dayton, Ohio.

References

1. S. H. McCracken and M. S. Salisbury, "Coherent 1.06 micron laser radar for fiber preamplifier research," in *SPIE LASERS '92 Conf., Proc. SPIE* **1633,** 86–93 (1992).
2. S. F. Carter, D. Szebesta, S. T. Davey, R. Wyatt, M. C. Brierley, and P. W. France, "Amplification at 1.3 μm in a PR^{3+}-doped single-mode fluorozirconate fiber," *Electron. Lett.* **27,** 628–629 (1991).
3. R. Olshansky, "Noise figure for erbium doped optical fibre amplifiers," *Electron. Lett.* **24,** 1363–1365 (1988).
4. P. W. France, *Optical Fibre Lasers & Amplifiers,* Blackie and Son Ltd., Glasgow and London (1991).
5. E. Snitzer, "Rare earth doped fiber lasers," in *Optical Fiber Commun. '92 Conf. Tutorial Sessions,* Tutorial FE, pp. 418–484, OSA, Washington, D.C. (Feb. 4–7, 1992).
6. R. E. Miers, "Fiber laser preamplifier for laser radar detectors," in *1991 USAF-RDL Summer Faculty Research Program Reports,* Vol. 5.B, Wright Laboratory Report 26, Wright-Patterson Air Force Base, Ohio (July 1991).
7. G. E. Keiser, *Optical Fiber Communications,* 2nd ed., p. 244, McGraw-Hill, Inc., New York (1991).
8. E. L. Dereniak and D. G. Crowe, *Optical Radiation Detectors,* John Wiley & Sons, New York (1984).
9. R. W. Boyd, *Radiometry and the Detection of Optical Radiation,* John Wiley & Sons, New York (1983).
10. W. L. Wolfe and G. J. Zissis, *The Infrared Handbook,* Table 21–3, Infrared Information and Analysis Center at Environmental Research Institute of Michigan, compiled for the Office of Naval Research, Department of the Navy (revised 1985).
11. R. H. Kingston, *Detection of Optical and Infrared Radiation,* Chap. 8, Springer-Verlag, New York (1978).
12. N. A. Olsson, "Lightwave systems with optical amplifiers," *J. Lightwave Technol.* **7**(7), 1071–1082 (1989).

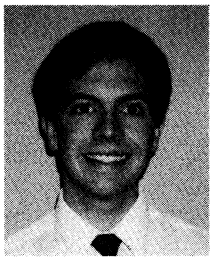

Michael S. Salisbury received BA degrees in physics and mathematics from North Central College in 1990. He obtained his MS degree in electro-optics from the University of Dayton while working as a research assistant at Wright-Patterson Air Force Base in the Wright Laboratory Electro-Optic Sensors Group (WL/AARI-2). In May of 1992, he was hired by Technology Scientific Services Incorporated, Dayton, Ohio, as a contractor assigned to the Wright Laboratory Electro-Optic Sensors facility. His research interests include optical fiber amplifiers, solid state ladar systems, ladar imaging, and remote sensing. Salisbury is a member of the Optical Society of America.

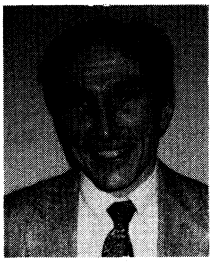

Paul F. McManamon received a BS degree in physics from John Carroll University. He then received MS and PhD degrees from Ohio State University in physics in 1977. Dr. McManamon has worked at Wright-Patterson Air Force Base since 1968. His initial work was in the area of designing countermeasure waveforms against microwave radars. He then moved into electro-optical countermeasures. In 1979 he took over the Thermal Imaging Group in the Air Force Avionics Laboratory and held that position for eight years. More recently he has been doing technical work in laser radar and passive electro-optical sensors. He is currently acting branch chief of the Electro-Optics Branch, Mission Avionics Division, Avionics Directorate of Wright Laboratory.

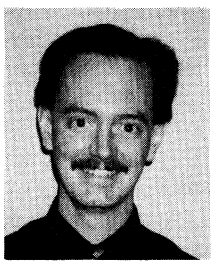

Bradley D. Duncan received the PhD degree in electrical engineering from Virginia Polytechnic Institute and State University (Virginia Tech) in 1991 and joined the University of Dayton faculty where he has since held the position of assistant professor of electrical engineering and electro-optics. His research interests and activities span a wide range of areas within the optical sciences, including the study of fiber optic sensor and system technology, integrated optics, acousto-optics, ladar imaging and system analysis, holography, and linear and nonlinear optical image processing. Dr. Duncan is a member of SPIE, the Optical Society of America, IEEE/Leos, and the American Society of Engineering Educators (ASEE).